HHS Public Access

Author manuscript

Bone. Author manuscript; available in PMC 2017 July 01.

Published in final edited form as:

Bone. 2016 July ; 88: 56–63. doi:10.1016/j.bone.2016.04.018.

T-type Voltage-Sensitive Calcium Channels Mediate Mechanically-Induced Intracellular Calcium Oscillations in Osteocytes by Regulating Endoplasmic Reticulum Calcium Dynamics

Genevieve N. Brown, **Pui L. Leong**, and **X. Edward Guo***

Bone Bioengineering Laboratory, Department of Biomedical Engineering, Columbia University, New York, NY 10027

Abstract

One of the earliest responses of bone cells to mechanical stimuli is a rise in intracellular calcium (Ca^{2+}), and osteocytes in particular exhibit robust oscillations in Ca^{2+} when subjected to loading. Previous studies implicate roles for both the endoplasmic reticulum (ER) and T-Type voltage-sensitive calcium channels (VSCC) in these responses, but their interactions or relative contributions have not been studied. By observing Ca^{2+} dynamics in the cytosol (Ca^{2+}_{cyt}) and the ER (Ca^{2+}_{ER}), the focus of this study was to explore the role of the ER and T-Type channels in Ca^{2+} signaling in bone cells. We demonstrate that inhibition of T-Type VSCC in osteocytes significantly reduces the number of Ca^{2+}_{cyt} responses and affects Ca^{2+}_{ER} depletion dynamics. Simultaneous observation of Ca^{2+} exchange among these spaces revealed high synchrony between rises in Ca^{2+}_{cyt} and depressions in Ca^{2+}_{ER}, and this synchrony was significantly reduced by challenging T-Type VSCC. We further confirmed that this effect was mediated directly through the ER and not through store-operated Ca^{2+} entry (SOCE) pathways. Taken together, our data suggests that T-Type VSCC facilitate the recovery of Ca^{2+}_{ER} in osteocytes to sustain mechanically-induced Ca^{2+} oscillations, uncovering a new mechanism underlying the behavior of osteocytes as mechanosensors.

Keywords

Osteocytes; calcium; endoplasmic reticulum; fluid flow; voltage-sensitive calcium channels

***Corresponding Author:** X. Edward Guo, Ph.D., Department of Biomedical Engineering, Columbia University, 351 Engineering Terrace, Mail Code 8904, 1210 Amsterdam Avenue, New York, NY 10027, U.S.A. ed.guo@columbia.edu, Telephone: 212-854-6196, Fax: 212-854-8725.

Conflicts of interest

All authors affirm that they have no conflicts of interest.

Authors' roles: XEG, PLL, and GNB conceptualized the study. GNB and PLL collected data. GNB drafted the manuscript. XEG and GNB interpreted the data. All authors approve the final version of the manuscript.

1. Introduction

Osteocytes are widely regarded as mechanosensors, capable of detecting changes in the mechanical environment of the bone tissue and modifying cellular responses accordingly[1,2]. Indeed, an intact osteocyte network is required for bone changes in response to unloading[3], and studies have shown that both loading and unloading influence osteocyte expression of proteins that modulate bone turnover[4], such as sclerostin[5,6] and receptor activator of nuclear factor kappa B ligand (RANKL)[7,8]. Still, mechanisms underlying osteocyte mechanotransduction remain unclear. For instance, one of the earliest responses of bone cells to mechanical stimuli is a rise in intracellular, or cytosolic, calcium (Ca^{2+}_{cyt}), but the mechanisms by which osteocytes generate or rely on Ca^{2+} signals to direct bone adaptation are largely unknown.

Osteocytes exhibit robust oscillations in Ca^{2+}_{cyt} in response to mechanical stimulation, a pattern distinct from their osteoblast precursors and attributed to their mechanosensitivity[9,10]. Prior *in vitro* work from our laboratory concluded that Ca^{2+}_{cyt} transients depend on both the extracellular reservoir of Ca^{2+} ions and intracellular storage organelles, in particular the endoplasmic reticulum (ER)[9]. Mechanically-induced ER Ca^{2+} (Ca^{2+}_{ER}) release depends on the purinergic pathway via inositol trisphosphate receptors (IP_3R) on the ER membrane. The release of Ca^{2+} from the ER is critical to fluid flow-induced Ca^{2+} oscillations in osteocytes; treatment with the drug thapsigargin to block ER Ca^{2+} reuptake significantly reduced the number of Ca^{2+}_{cyt} transients from an average of five down to a single response. A similar effect was observed in *in situ* osteocytes, where thapsigargin treatment abolished multiple Ca^{2+} responses induced by dynamic loading of a murine tibia[10].

Ca^{2+}_{cyt} oscillations in osteocytes are also affected by inhibition of a number of membrane channels involved in Ca^{2+} transport, and targeting channels expressed primarily in osteocytes should clarify some mechanisms underlying this unique behavior. For instance, the expression of voltage-sensitive calcium channel (VSCC) subtypes changes as osteoblasts differentiate into osteocytes[11]. Osteoblasts express both low threshold T- and high threshold L-type VSCC, whereas osteocytes predominantly express T-Type VSCC[12]. Previous studies published from our laboratory explored the effects of VSCC inhibitors when added to the flow medium after shear stimulation9. The addition of the T-Type inhibitor NNC 55-0396 interrupted Ca^{2+}_{cyt} responses in osteocytes, preventing subsequent Ca^{2+} transients, but had little observable effect on osteoblasts. Treatment of *in situ* osteocytes with the T-Type inhibitor prior to mechanical stimulation also significantly reduced the number of Ca^{2+} responses[10]. Interestingly, inhibition of these channels in both systems had similar effects as disruption of ER stores, though no link has been demonstrated between them in osteocytes.

VSCC have been shown to interact with the ER and Ca^{2+}_{ER} release pathways in other cells. A direct association of T-Type VSCC with the ER has been previously demonstrated in arterial smooth muscle, where $Ca_V3.2$ channels were found to be localized to ER caveolae by transmission electron microscopy and to bind to ryanodine receptors on the ER by a proximity ligation assay[13]. In addition, a number of proteins participate in Ca^{2+} release from ER stores and Ca^{2+} entry triggered by this release – a phenomenon referred to as store-

operated calcium entry (SOCE) – such as Stromal Interaction Molecules (STIMs) and Ca^{2+}-Release Activated Channels (CRACs)[14]. In particular, STIM1 has been shown to interact with L-Type VSCC in rat cortical neurons15 and vascular smooth muscle cells[16] and $Ca_V3.1$ T-Type VSCC in cardiac myocytes[17]. The potential role of SOCE-related proteins in osteocyte Ca^{2+} signaling have not yet been explored.

Though our previous studies implicate roles for both the ER and T-Type VSCC in osteocyte Ca^{2+}_{cyt} responses, their relative contributions or any interactions between the ER and T-Type VSCC remain unknown. This is largely due to an inability to monitor Ca^{2+} localized to the ER separately from Ca^{2+} entering the cell from the extracellular fluid. However, advances in genetically encoded Ca^{2+} biosensors now enable the targeting of these sensors to subcellular organelles, including the ER[18–20].

Thus, the focus of the current study is to observe Ca^{2+}_{ER} dynamics in bone cells to better understand the role of ER stores in the unique Ca^{2+} oscillations in osteocytes. We hypothesized that an ability to refill ER stores results in Ca^{2+}_{cyt} oscillations in osteocytes. We also hypothesized that the predominant expression of T-type channels in osteocytes may contribute to their unique Ca^{2+}_{cyt} patterns and further speculated that T-type VSCC in osteocytes may interact with ER stores.

2. Materials and Methods

2.1 Cell culture

Osteocyte-like MLO-Y4 cells (a gift from Dr. Lynda Bonewald, University of Missouri-Kansas City, Kansas City, MO) were cultured on 0.15 mg/ml collagen (rat tail type I, BD Biosciences, San Jose, CA) coated culture dishes in minimum essential alpha medium (α-MEM, Life Technologies, Carlsbad, CA) supplemented with 5% fetal bovine serum (FBS, Hyclone Laboratories Inc., Logan, UT) and 5% calf serum (CS, Life Technologies, Carlsbad, CA). MC3T3-E1 pre-osteoblasts (ATCC, Manassas, VA) were cultured in α-MEM supplemented with 10% FBS. Cells were maintained at 5% CO_2 and 37°C in a humidified incubator. MLO-Y4 cells were sub-cultured prior to reaching 70–80% confluence in order to maintain an osteocyte-like phenotype.

2.2 Immuno-detection

To detect the presence of L- and T-Type VSCC in osteocytes and osteoblasts, we performed Western blots and immunostaining using antibodies targeted against $Ca_V1.2$ (L-Type) and $Ca_V3.2$ (T-Type) subunits (SDIX, Newark, DE). Protein was extracted from monolayer cell cultures using RIPA lysis buffer with protease and phosphatase inhibitors (Roche Diagnostics, Indianapolis, IN). Western blots were performed on MLO-Y4 and MC3T3-E1 lysates of equal total protein as determined by a BCA assay (Pierce, ThermoFisher Scientific, Waltham, MA). For immunostaining, cells were fixed in 4% paraformaldehyde and permeabilized with 2% Triton™ X-100 (Sigma-Aldrich, St. Louis, MO). Following antibody incubations, cells were counterstained with DAPI to label nuclei (Molecular Probes, Eugene, OR).

2.3 Inhibitors

All inhibitors used in this study were purchased from Sigma-Aldrich (St. Louis, MO). Thapsigargin is an inhibitor of the Ca^{2+}-ATPase pump on the ER (SERCA) which facilitates the reuptake of Ca^{2+} into the ER, and thapsigargin treatment (1μM) thereby results in ER depletion. Two VSCC inhibitors were used in this study: the T-Type inhibitor NNC 55-0396 (20 μM) and the L-Type specific inhibitor nifedipine (10μM). MLO-Y4 cells were also treated with the following inhibitors related to SOCE: YM58483 (3μM), a CRAC inhibitor[21]; SKF-96365 (50μM), a SOCE inhibitor that inhibits STIM1 (similar effects as STIM1 silencing)[22] but exhibits off-target effects on VSCC activity[23]; and 2-APB (50μM), a reliable inhibitor of SOCE and IP_3R[23,24]. Cells were incubated in the inhibitors for 15 minutes prior to flow exposure, and the inhibitors remained in the flow medium for the duration of the experiment.

2.4 Ca^{2+}_{cyt} indicators and Ca^{2+}_{ER} visualization

To observe Ca^{2+}_{cyt} changes only, MLO-Y4 and MC3T3-E1 cells were stained with Fluo-8 AM (AAT Bioquest, Sunnyvale, CA) dissolved in 20% Pluronic F-127 in DMSO (Invitrogen, Carlsbad, CA). To visualize ER calcium levels in osteocytes and osteoblasts, cells were transiently transfected with the D1ER plasmid (plasmid #36325, Addgene, Cambridge, MA)[25] using standard non-liposomal techniques (Fugene 6, Promega Corporation, Madison, WI). D1ER is a second generation cameleon Ca^{2+} fluorescence resonance energy transfer (FRET) sensor targeted to the ER with a retention sequence. To simultaneously visualize Ca^{2+}_{cyt} and Ca^{2+}_{ER}, cells were transfected with D1ER and then stained with the red-shifted Ca^{2+}_{cyt} indicator Fura Red-AM (20μM, Life Technologies, Carlsbad, CA) in DMSO and Kolliphor® EL (Sigma-Aldrich, St. Louis, MO) prior to fluid flow stimulation.

To verify the localization of the D1ER plasmid, transfected cells were stained with ER-Tracker Red (Molecular Probes, Eugene, OR). Cells were rinsed and incubated with a warmed 1μM working solution of ER-Tracker Red for 30 minutes at 37°C. Cells were rinsed with fresh medium and post-incubated for 15 minutes prior to imaging. The FRET biosensor was excited at 430nm, and fluorescence emission of YFP (530nm) was collected as the FRET image. The ER Tracker Red dye was imaged using 568nm excitation/660nm emission.

2.5 Fluid flow stimulation

Prior to staining with appropriate Ca^{2+} indicators, cells were plated onto 10μg/mL fibronectin-coated glass slides at ~80% confluency to establish cell-cell contact. Slides were then stained and assembled into a custom parallel-plate flow chamber with a glass bottom that permits live cell imaging under fluid shear stimulation. The chamber was placed on the stage of an inverted microscope (Olympus, Waltham, MA) and attached to a magnetic gear pump (Scilog, Madison, WI) for the application of steady, laminar, unidirectional flow at a shear stress of 35 dynes/cm^2, which has been shown to induce multiple Ca^{2+}_{cyt} responses in osteocytes and fewer, weaker responses in osteoblasts in our previous studies[9]. In addition, the Ca^{2+}_{cyt} patterns observed *in vitro* under this flow profile are consistent with those observed in *ex vivo* mouse tibia under physiologic dynamic loads[10], while oscillatory flow

induces fewer responses[26]. Baseline fluorescence intensity was captured for 1 minute prior to fluid shear stimulation for 9 minutes.

2.6 Imaging and image analysis

For monitoring ER depletion, time-lapse images were collected 36–48 hours post transfection at 40× magnification. The FRET biosensor was excited at 430nm, and fluorescence emissions of YFP (530nm) and CFP (470nm) were captured simultaneously using a quadview beamsplitter and custom quad-band polychroic[27]. To monitor ER depletion, cells were imaged for 20 minutes following the addition of thapsigargin (1μM). Images were acquired every 3 seconds to minimize photobleaching. The FRET ratio was calculated on a pixel-by-pixel basis using cross-correlation based image registration of the FRET and donor emissions to obtain relative Ca^{2+}_{ER} levels. The time to depletion was defined as the time at which the normalized FRET ratio fell below 0.8[28].

To monitor the effects of VSCC and SOCE inhibitors on Ca^{2+}_{cyt} responses, time-lapse images of cells were collected at 20× magnification for 9 minute periods of fluid flow stimulation. The Fluo-8 Ca^{2+} indicator was excited at 488nm, and fluorescence emissions were collected at 527nm. A Ca^{2+}_{cyt} transient was defined by an increase Fluo-8 intensity at least 4 times the magnitude of noise prior to flow onset[29].

To simultaneously monitor Ca^{2+}_{cyt} and Ca^{2+}_{ER}, single cells expressing Fura Red and the D1ER FRET sensor were identified at 60× magnification. Single excitation (430nm) was used to excite the dye and FRET biosensor, and fluorescence emissions of YFP, CFP, and Fura Red (641nm) were captured separately and simultaneously. Images were acquired every 3 seconds. Ca^{2+}_{cyt} time-courses were extracted from the Fura Red image. Photobleaching was corrected in this channel using an exponential fit of the baseline Ca^{2+}_{cyt} levels. The FRET ratio was determined from registered FRET/donor emissions. Regions of interest were selected to capture Ca^{2+} micro-domains within the cell based on the location of the initiation of a Ca^{2+}_{cyt} response[30]. To investigate the relationship between Ca^{2+} activity in the cytosol and the ER, we defined a percentage synchrony as the number of coincident Ca^{2+}_{cyt} and Ca^{2+}_{ER} transients divided by the total number of transients (peaks and inverse peaks). Ca^{2+}_{cyt} peaks and decreases in Ca^{2+}_{ER} were identified as transient responses (i.e. decrease and recovery) with a magnitude greater than four times the magnitude of the noise in the baseline images.

2.7 Data analysis

The data presented herein analyzes only responsive cells, though responsive percentages were greater than 80% for all experiments, except for SKF-96365 and 2-ABP treatment, which reduced the number of responsive MLO-Y4 cells to ~60% and 50%, respectively in cell populations. A cell was defined as responsive if the magnitude of the first Ca^{2+}_{cyt} response was at least four times higher than fluctuations in intensity during baseline measurements. Student's t-tests were used to determine significant differences for the number of Ca^{2+}_{cyt} peaks at a specific experimental condition. All data are shown as mean ± standard deviation. Multi-factorial analysis of variance (ANOVA) with Bonferroni's post hoc analysis was performed to determine statistical differences between mean values of

inhibitor treatments on the two cell types. Statistical significance can be observed when $p<0.05$.

3. Results

3.1 Expression of L- and T-Type VSCC in osteocytes and osteoblasts

MLO-Y4 cells express little to no detectable L-Type protein by Western blot and little protein by immunohistochemistry (Fig. 1A). T-Type expression, on the other hand, is abundant in both protein extracts and fixed cells. MC3T3-E1 cells express both L- and T-Type proteins in similar abundance (Fig. 1B).

3.2 Effects of L- and T-Type VSCC inhibitors on bone cell Ca^{2+}_{cyt} responses to fluid flow

Osteocytes (n=480 cells, 18 slides) exhibited numerous Ca^{2+}_{cyt} oscillations under fluid flow, and these multiple responses were significantly reduced by treatment with the T-type inhibitor NNC 55-0396 (n= 201 cells, 10 slides) (Fig. 2A). The L-type inhibitor had no effect on the number of Ca^{2+}_{cyt} responses in osteocytes (n=187 cells, 8 slides). Osteoblasts were less responsive than osteocytes, exhibiting less than two Ca^{2+}_{cyt} peaks on average for all groups (n=237, 53, 79 cells; 8, 2, 3 slides for control, L- and T-Type inhibitors, respectively) (Fig. 2B).

3.3 Effects VSCC inhibitors on ER dynamics in bone cells

The localization of the D1ER plasmid to the ER was verified by staining D1ER-transfected osteocytes with ER Tracker Red (Fig. 3A). Transfected cells were imaged for 20 minutes following the addition of thapsigargin to deplete the ER. Representative FRET ratios of a single osteocyte treated with thapsigargin is shown in Fig. 3B.

The time to deplete the ER under the outlined conditions is shown in Fig. 3C and D. The scatter plots show representative depletion curves for MLO-Y4 cells (Fig. 3C) and MC3T3-E1 cells (Fig. 3D). The small difference (3%) between untreated MLO-Y4 cells (n=14) and MC3T3-E1 cells (n=6) in the time to depletion did not reach significance. Similarly, the effect of VSCC inhibitors had on the time to depletion in osteoblasts was not significant (Fig. 3D; n=5, 4 cells for L- and T-Type inhibition, respectively), and the L-Type VSCC inhibitor had no effect in osteocytes (Fig. 3C, n=5 cells). Treatment of MLO-Y4 cells with the T-Type VSCC inhibitor prior to the addition of thapsigargin resulted in a significantly faster time to depletion compared to untreated controls (Fig. 3C, n=6 cells). On average, it took ~300s longer for Ca^{2+}_{ER} levels to deplete in control cells than those with disrupted T-Type VSCC.

3.4 Simultaneous imaging of Ca^{2+}_{cyt} and Ca^{2+}_{ER} in bone cells under fluid flow

To simultaneously image Ca^{2+}_{cyt} and Ca^{2+}_{ER}, bone cells were transfected with D1ER, stained with Fura Red-AM, and imaged using a quadview beamsplitter (Fig. 4A). The FRET ratio was calculated from the FRET and donor images, and in some cells, a subregion corresponding to Ca^{2+}_{cyt} spike initiation was selected for analysis (Fig. 4B). Representative time courses for MLO-Y4 and MC3T3-E1 cells under control (untreated), L-Type inhibitor treated, and T-Type inhibitor treated conditions is shown in Fig. 4C. In osteocytes, elevations

of Ca^{2+}_{cyt} coincided with depression of Ca^{2+}_{ER}, with subsequent peaks occurring after recovery of Ca^{2+}_{ER} levels (n=10 cells). In osteoblasts, significantly fewer Ca^{2+}_{cyt} responses were observed, and while the ER contributed to these responses, a depression in Ca^{2+}_{ER} was often not recovered in the course of the experiment (n=11 cells). Treatment of either cell type with the L-Type VSCC inhibitor nifedipine had no detectable effect on the number of Ca^{2+}_{cyt} peaks (n=8 osteocytes, 5 osteoblasts), and the T-Type VSCC inhibitor NNC 55-0396 had no detectable effect on responses in osteoblasts (n=6 cells). Treatment of MLO-Y4 cells with the T-Type VSCC inhibitor significantly reduced the number of Ca^{2+}_{cyt} responses (Fig. 4D, n=9 cells).

The percentage of synchronous responses was defined as the number of coincident Ca^{2+}_{cyt} and Ca^{2+}_{ER} transients divided by the total number of transients (peaks and inverse peaks). The synchronous response percentage was high in control osteocytes, with more than 80% of Ca^{2+}_{cyt} peaks corresponding to dynamic changes in Ca^{2+}_{ER} (Fig. 4E). MC3T3-E1 cells exhibited few Ca^{2+}_{cyt} peaks in response to flow (Fig. 4D), and more often than not those peaks were not synchronous with a transient drop in Ca^{2+}_{ER} (Fig. 4E). Inhibition of T-Type VSCC significantly reduced the synchrony in osteocytes to similar levels observed in osteoblasts, with an average of ~20%.

3.5 Effects of SOCE inhibitors on osteocyte Ca^{2+}_{cyt} responses

MLO-Y4 cells were subjected to fluid flow stimulation in the presence of three different SOCE-related inhibitors to inform the mechanism of Ca^{2+} exchange with the ER. The number of Ca^{2+}_{cyt} peaks (Fig. 5A) and the synchronous response percentage (Fig. 5B) were determined for each group. YM58483 had no effect on Ca^{2+}_{cyt} responses in osteocytes (n=3 cells), and though SKF-96365 reduced the number of Ca^{2+}_{cyt} responses, the effect was not significant (n=4 cells). This trend was consistent with population studies (YM58483: n=223 cells, 7 slides; SKF-96365: n=231 cells, 4 slides; data not shown). Neither treatment influenced synchrony. Treatment with 2-APB significantly reduced the number of Ca^{2+}_{cyt} responses and the percent of synchronous responses (n=5 cells). Again, the effect on Ca^{2+}_{cyt} responses was consistent with Fluo-8 experiments on larger cell populations (n=84 cells, 5 slides; data not shown). Representative curves of Ca^{2+}_{cyt} and Ca^{2+}_{ER} in MLO-Y4 cells treated with these inhibitors showed high synchrony in YM58483 and SKF-96365 treated cells (Fig. 5C,D), whereas 2-APB treatment resulted in no recovery of ER levels following a Ca^{2+}_{cyt} transient (Fig. 5E).

4. Discussion

The purpose of this study was to uncover mechanisms underlying the generation of Ca^{2+}_{cyt} oscillations in osteocytes. Previous studies have implicated the ER as an important source of Ca^{2+} for transient Ca^{2+} signals in osteocytes responding to mechanical stimuli, however to date no study has precisely identified the mechanisms by which the ER enables Ca^{2+}_{cyt} oscillations in osteocytes. This study represents the first attempt to visualize the dynamics of Ca^{2+} specifically in the ER in osteocytes. Using a FRET biosensor localized to the ER, we were able to simultaneously observe Ca^{2+} exchange between the ER and the cytosol. We found high synchrony between rises in Ca^{2+}_{cyt} and depressions in Ca^{2+}_{ER}, with subsequent

Ca^{2+}_{cyt} responses occurring after a recovery of Ca^{2+}_{ER} levels, suggesting that ER dynamics dictate osteocyte Ca^{2+} responses to fluid flow. Additionally, a major goal of this study was to link a phenotypic difference between osteocytes and osteoblasts in the expression of VSCC to the mechanobiology of these cell types. Indeed, we found that challenging T-Type VSCC alters the kinetics of ER depletion in osteocytes and that the predominant expression of T-Type VSCC in osteocytes sustains Ca^{2+}_{cyt} oscillations by facilitating $Ca^{2+}_{cyt}/Ca^{2+}_{ER}$ synchrony. Using inhibitors of various SOCE-related pathways, we determined that this exchange of Ca^{2+} between the cytosol and the ER is likely not a result of STIM proteins or transport of Ca^{2+} through CRACs, but rather through an interaction of the ER with T-Type channels on the osteocyte cell membrane.

Previous studies detected little to no L-Type VSCC expression in MLO-Y4 osteocytes, but found detectable levels of T-Type VSCC[11]. Furthermore, a pattern of development suggested a loss of L-Type VSCC with the differentiation of osteoblasts to osteocytes. A later study confirmed this finding and additionally reported that T-Type channels mediated mechanically-induced ATP release in osteocytes[12]. Most recently, a study in IDG-SW3 osteocytes found that parathyroid hormone treatment increased the expression of L-Type VSCC and decreased T-Type VSCC in osteocyte-stage cells to revert them to a less mature phenotype[31]. Our results are consistent with the role of VSCC in the differentiation of osteoblasts to osteocytes and additionally suggest the predominant expression of T-Type VSCC in osteocytes is important for their distinct role as mechanosensors.

As previous studies resulted in similar effects of VSCC and ER antagonists on osteocyte Ca^{2+}_{cyt} responses, we sought to determine whether there was any interaction between T-Type VSCC and the ER in osteocytes. The time to depletion was very similar (within 3%) in untreated MLO-Y4 and MC3T3-E1, suggesting that ER release kinetics alone cannot account for the Ca^{2+}_{cyt} oscillation behavior in osteocytes. Treatment of MLO-Y4 with a T-Type VSCC inhibitor prior to thapsigargin resulted in a significantly faster time to depletion compared to untreated controls. This suggests that the presence of T-Type VSCC may serve to refill ER stores in osteocytes, which may explain the ability of osteocytes to sustain Ca^{2+}_{cyt} oscillations.

Though inhibitor studies challenging the ER allude to a mechanism involving Ca^{2+}_{ER} release and refilling in sustaining Ca^{2+}_{cyt} oscillations in osteocytes, these conclusions are speculative without the direct measurement of Ca^{2+}_{ER} dynamics under flow. This is also true for measurements of ER depletion, where only a single induction of Ca^{2+}_{ER} release is monitored. In this study, by simultaneously monitoring Ca^{2+} separately in the cytosol and ER in osteocytes, we found that most rises in Ca^{2+}_{cyt} were accompanied by a corresponding decrease and recovery in Ca^{2+}_{ER}. This supports the hypothesis that osteocytes are capable of generating Ca^{2+}_{cyt} oscillations by an ability to refill the ER stores. The effects of T-Type VSCC inhibition implicate T-Type channels in this process.

Though the T-Type inhibitor had a large suppressive effect on $Ca^{2+}_{cyt}/Ca^{2+}_{ER}$ synchrony in osteocytes, there are other possible mechanisms linking the exchange of Ca^{2+} between these two spaces. However, the lack of a pronounced suppression between control cells and those treated with YM58483 on the number of Ca^{2+}_{cyt} responses and the percentage of

synchronous responses indicates that CRACs are not involved. While SKF-96365 treatment mildly decreased the number of responses, this reduction is likely due to reported off-target effects on VSCC[23]. The only inhibitor that produced similar effects as the T-Type antagonist was the IP_3R inhibitor 2-APB, which blocks IP_3-mediated release of Ca^{2+} from the ER. Thus, the exchange of Ca^{2+} between the cytosol and the ER is likely not a result of Ca^{2+} transport through CRAC or STIM1 involvement, but rather through the IP_3-mediated release of Ca^{2+}_{ER}. Taken together, this data suggests that T-Type VSCC may directly interact with the ER in osteocytes, with the ER possibly relying on T-Type VSCC to replenish Ca^{2+} following Ca^{2+} release into the cytosol. Indeed, in cerebral arteries, the association of T-Type $Ca_V3.2$ with Ca^{2+}_{ER} transporters drove RyR-mediated Ca^{2+} sparks[13]. Thus, it is possible a similar interaction exists between T-Type VSCC and ER-mediated Ca^{2+} oscillations in osteocytes.

There are a few limitations to the current study. First, the small sample sizes, though consistent with our experiments on large cell populations, mean our study was only designed to detect relatively large effects of the investigated treatments. Future studies looking for more subtle differences will require a larger sample size. In addition, our conclusions are drawn from experiments using small molecule inhibitors, which often have incomplete or off-target effects. Thus, future studies will be aimed at genetic modifications of cells to alter the expression of VSCC to investigate their role in osteocyte Ca^{2+} signaling. Furthermore, the simultaneous observation of Ca^{2+}_{ER} levels in cells challenged with VSCC inhibitors only alludes to their interactions; true association of these structures will need to be verified by a proximity ligation or pull-down assay. Finally, the average synchrony in osteoblasts was also approximately 20%, though standard deviations were somewhat high due to the limited number of responses. As all T-Type treated MC3T3-E1 cells analyzed in this study had only one response with no coincident inverse response from the ER, the synchrony in the T-Type treated osteoblasts was zero, though this value was still not statistically different from MC3T3-E1 untreated controls. Although the present study indicates that the first Ca^{2+}_{cyt} response in both cells can have some contribution of the ER, it is known that extracellular Ca^{2+} is also required, thus this effect is likely due to differences between the first and subsequent Ca^{2+}_{cyt} transients in these cells. Future work will aim to explore these differences.

5. Conclusions

The sustainment of robust oscillations in Ca^{2+}_{cyt} under mechanical loading is a hallmark of osteocytes both *in vitro* and *ex vivo*, thus the primary goal of this study was to uncover the mechanism by which osteocytes rely on specific subcellular stores of Ca^{2+} to generate these multiple responses. By observing Ca^{2+} dynamics in both cytosolic and ER spaces, this study demonstrated that osteocytes generate multiple responses through an ability to refill ER stores. Our data suggests that T-type VSCC facilitate the recovery of Ca^{2+}_{ER} in osteocytes to permit this behavior. We uncovered a new mechanism involving T-type VSCC underlying the unique behavior of osteocytes as mechanosensors.

Acknowledgments

We thank Dr. Lynda Bonewald for her generous gift of MLO-Y4 cells and Amy Palmer and Roger Tsien for kindly providing the D1ER plasmid.

This work was supported by NIH R01 AR 052641. GNB was supported by the National Science Foundation Graduate Research Fellowship Program.

Abbreviations

ER	Endoplasmic reticulum
VSCC	voltage-sensitive calcium channels
Ca^{2+}	calcium
SOCE	store-operated calcium entry
IP_3	inositol trisphosphate

References

1. Bonewald LF. The amazing osteocyte. J Bone Miner Res. 2011; 26:229–238. [PubMed: 21254230]
2. Schaffler MB, Cheung W-Y, Majeska R, Kennedy O. Osteocytes: Master Orchestrators of Bone. Calcif Tissue Int. 2014; 94:5–24. [PubMed: 24042263]
3. Tatsumi S, et al. Targeted Ablation of Osteocytes Induces Osteoporosis with Defective Mechanotransduction. Cell Metabolism. 2007; 5:464–475. [PubMed: 17550781]
4. Lara-Castillo N, et al. In vivo mechanical loading rapidly activates β-catenin signaling in osteocytes through a prostaglandin mediated mechanism. Bone. 2015; 76:58–66. doi:http://dx.doi.org/10.1016/j.bone.2015.03.019. [PubMed: 25836764]
5. Compton JT, Lee FY. A Review of Osteocyte Function and the Emerging Importance of Sclerostin. 2014; 96:1659–1668.
6. Robling AG, et al. Mechanical Stimulation of Bone in Vivo Reduces Osteocyte Expression of Sost/Sclerostin. Journal of Biological Chemistry. 2008; 283:5866–5875. [PubMed: 18089564]
7. Nakashima T, et al. Evidence for osteocyte regulation of bone homeostasis through RANKL expression. Nature medicine. 2011; 17:1231–1234.
8. Xiong J, et al. Matrix-embedded cells control osteoclast formation. Nature medicine. 2011; 17:1235–1241.
9. Lu XL, Huo B, Chiang V, Guo XE. Osteocytic network is more responsive in calcium signaling than osteoblastic network under fluid flow. J Bone Miner Res. 2012; 27:563–574. [PubMed: 22113822]
10. Jing D, et al. In situ intracellular calcium oscillations in osteocytes in intact mouse long bones under dynamic mechanical loading. The FASEB Journal. 2014; 28:1582–1592. [PubMed: 24347610]
11. Shao Y, Alicknavitch M, Farach-Carson MC. Expression of voltage sensitive calcium channel (VSCC) L-type Cav1.2 (α1C) and T-type Cav3.2 (α1H) subunits during mouse bone development. Developmental Dynamics. 2005; 234:54–62. [PubMed: 16059921]
12. Thompson WR, et al. Association of the alpha(2)delta(1) subunit with Ca(v)3.2 enhances membrane expression and regulates mechanically induced ATP release in MLO-Y4 osteocytes. J Bone Miner Res. 2011; 26:2125–2139. [PubMed: 21638318]
13. Harraz OF, et al. CaV3.2 Channels and the Induction of Negative Feedback in Cerebral Arteries. Circulation Research. 2014; 115:650–661. [PubMed: 25085940]
14. Smyth JT, et al. Activation and regulation of store-operated calcium entry. Journal of Cellular and Molecular Medicine. 2010; 14:2337–2349. [PubMed: 20807283]

15. Park CY, Shcheglovitov A, Dolmetsch R. The CRAC Channel Activator STIM1 Binds and Inhibits L-Type Voltage-Gated Calcium Channels. Science. 2010; 330:101–105. [PubMed: 20929812]
16. Wang Y, et al. The Calcium Store Sensor, STIM1, Reciprocally Controls Orai and CaV1.2 Channels. Science. 2010; 330:105–109. [PubMed: 20929813]
17. Nguyen N, et al. STIM1 participates in the contractile rhythmicity of HL-1 cells by moderating T-type Ca2 + channel activity. Biochimica et Biophysica Acta (BBA) - Molecular Cell Research. 2013; 1833:1294–1303. doi:http://dx.doi.org/10.1016/j.bbamcr.2013.02.027. [PubMed: 23458835]
18. Suzuki J, et al. Imaging intraorganellar Ca2+ at subcellular resolution using CEPIA. Nat Commun. 2014; 5
19. Costantini L, Snapp E. Probing Endoplasmic Reticulum Dynamics using Fluorescence Imaging and Photobleaching Techniques. Current Protocols in Cell Biology. 2001 <http://dx.doi.org/10.1002/0471143030.cb2107s60>.
20. Palmer AE, et al. Ca2+ indicators based on computationally redesigned calmodulin-peptide pairs. Chemistry & biology. 2006; 13:521–530. [PubMed: 16720273]
21. Ishikawa J, et al. A Pyrazole Derivative, YM-58483, Potently Inhibits Store-Operated Sustained Ca2+ Influx and IL-2 Production in T Lymphocytes. The Journal of Immunology. 2003; 170:4441–4449. [PubMed: 12707319]
22. Chen Y-T, et al. The ER Ca2+ sensor STIM1 regulates actomyosin contractility of migratory cells. Journal of cell science. 2013; 126:1260–1267. [PubMed: 23378028]
23. Jairaman A, Prakriya M. Molecular pharmacology of store-operated CRAC channels. Channels. 2013; 7:402–414. [PubMed: 23807116]
24. Bootman MD, et al. 2-Aminoethoxydiphenyl borate (2-APB) is a reliable blocker of store-operated Ca2+ entry but an inconsistent inhibitor of InsP3-induced Ca2+ release. The FASEB Journal. 2002; 16:1145–1150. [PubMed: 12153982]
25. Palmer AE, Jin C, Reed JC, Tsien RY. Bcl-2-mediated alterations in endoplasmic reticulum Ca2+ analyzed with an improved genetically encoded fluorescent sensor. Proceedings of the National Academy of Sciences of the United States of America. 2004; 101:17404–17409. [PubMed: 15585581]
26. Lu XL, Huo B, Park M, Guo XE. Calcium response in osteocytic networks under steady and oscillatory fluid flow. Bone. 2012; 51:466–473. [PubMed: 22750013]
27. Baik AD, et al. Quasi-3D Cytoskeletal Dynamics of Osteocytes under Fluid Flow. Biophysical Journal. 2010; 99:2812–2820. [PubMed: 21044578]
28. Hara T, et al. Calcium Efflux From the Endoplasmic Reticulum Leads to β-Cell Death. Endocrinology. 2014; 155:758–768. doi:doi:10.1210/en.2013-1519. [PubMed: 24424032]
29. Donahue SW, Donahue HJ, Jacobs CR. Osteoblastic cells have refractory periods for fluid-flow-induced intracellular calcium oscillations for short bouts of flow and display multiple low-magnitude oscillations during long-term flow. Journal of Biomechanics. 2003; 36:35–43. [PubMed: 12485636]
30. Lee K, et al. The primary cilium functions as a mechanical and calcium signaling nexus. Cilia. 2015; 4:7. [PubMed: 26029358]
31. Prideaux M, et al. Parathyroid Hormone Induces Bone Cell Motility and Loss of Mature Osteocyte Phenotype through L-Calcium Channel Dependent and Independent Mechanisms. PloS one. 2015; 10:e0125731. [PubMed: 25942444]

Highlights

- Ca^{2+}_{cyt} and Ca^{2+}_{ER} are observed simultaneously in single bone cells under flow.
- Ca^{2+} exchange between the ER and the cytosol is highly synchronized in osteocytes.
- Antagonizing T-Type VSCC in osteocytes alters Ca^{2+}_{ER} dynamics and synchrony.

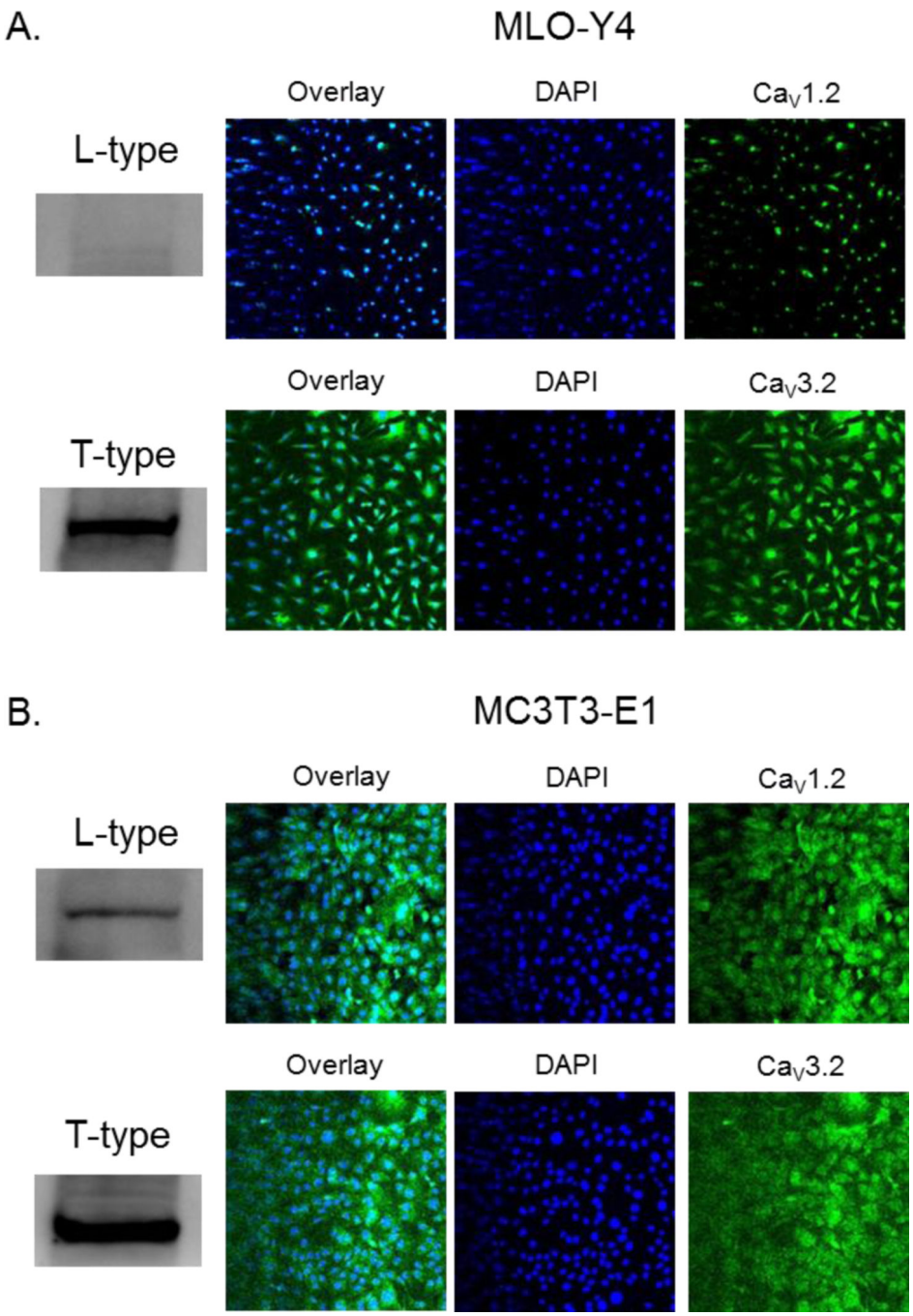

Figure 1. The expression of L- and T-Type VSCC in MLO-Y4 osteocytes and MC3T3-E1 osteoblasts

Immuno-detection of L- and T-Type VSCC proteins from whole cell lysates (Western blot) and in fixed cell populations of (A) MLO-Y4 and (B) MC3T3-E1 cells.

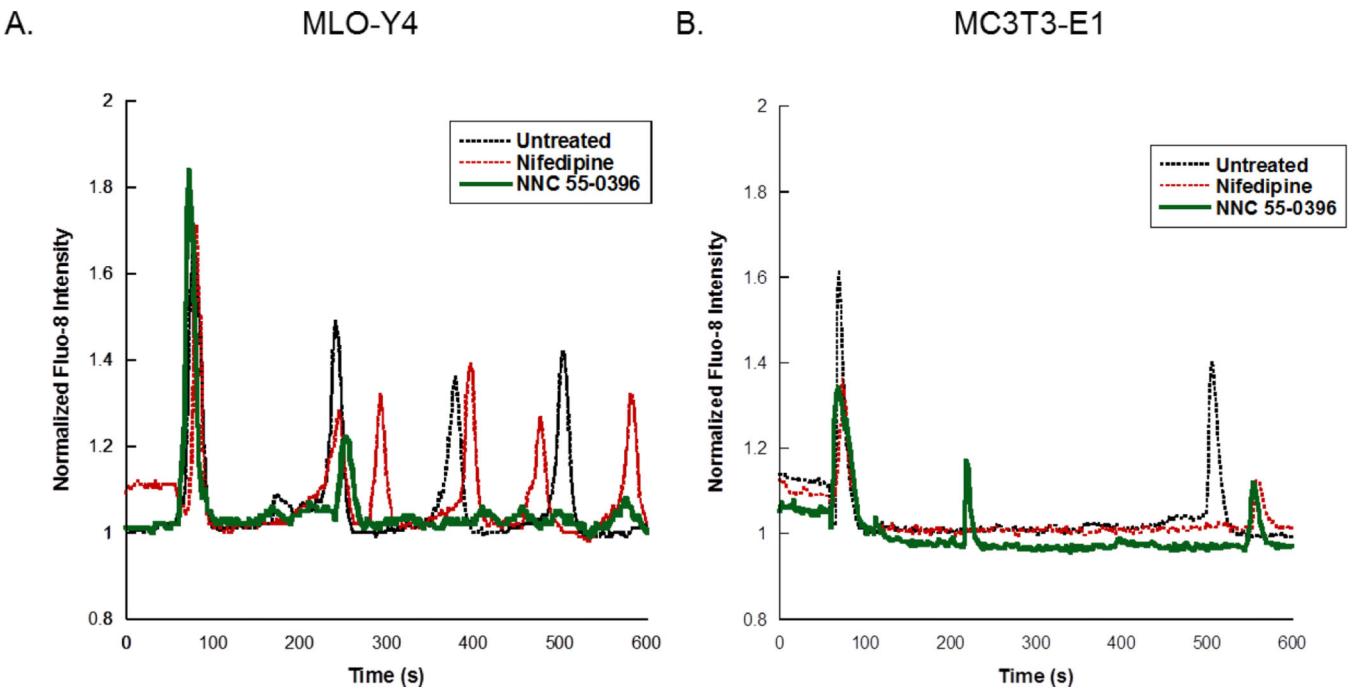

Figure 2. The effects of VSCC inhibitors on Ca2+cyt responses in osteocytes and osteoblasts

Representative Ca^{2+}_{cyt} time courses are shown for (A) MLO-Y4 and (B) MC3T3-E1 cells treated with the L-Type inhibitor nifedipine or the T-Type inhibitor NNC 55-0396 prior to exposure to fluid flow. Ca^{2+}_{cyt} transients are shown as intensity changes of the fluorescent indicator Fluo-8 normalized to intensity at baseline prior to fluid flow exposure.

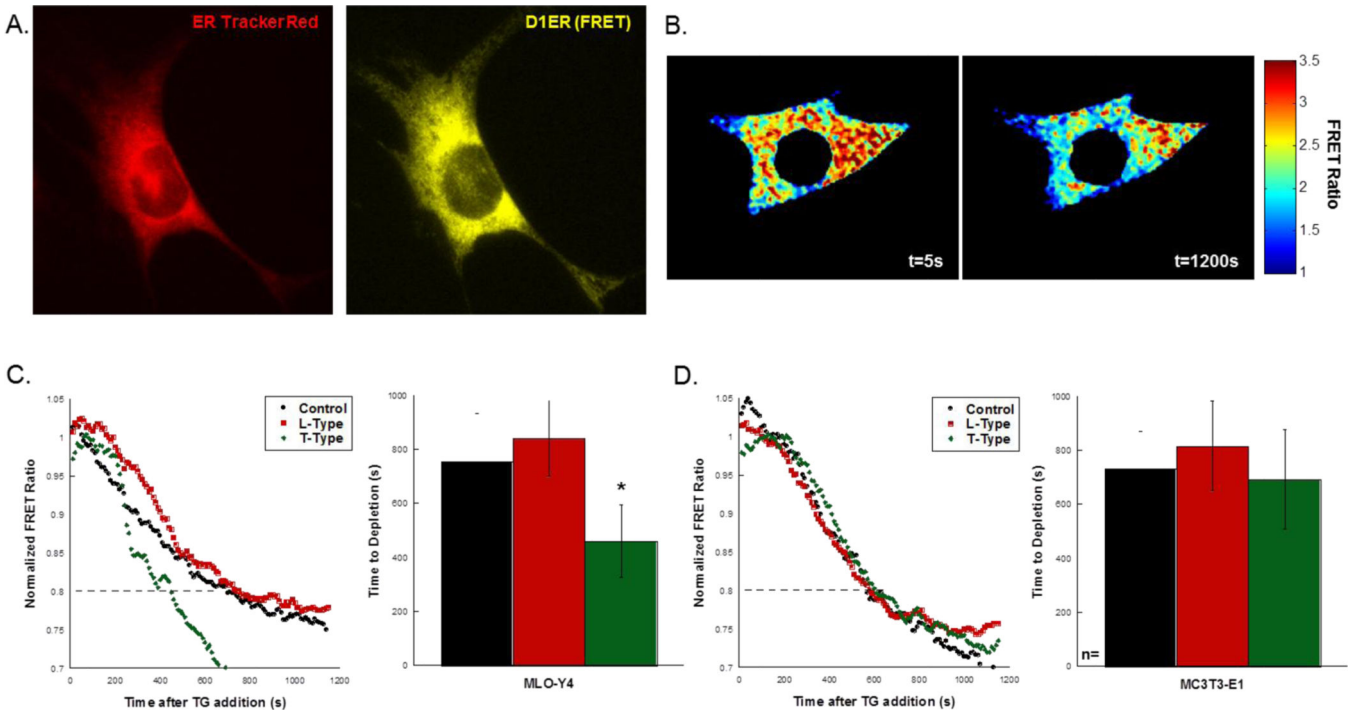

Figure 3. The effects of VSCC inhibitors on Ca^{2+} dynamics in the ER

(A) Ca^{2+}_{ER} was indicated by transfect of cells with the D1ER plasmid (yellow = FRET), which localizes to the ER. Images were collected at 40× magnification. (B) Thapsigargin was used to induce depletion of the ER over the time course of the experiment. The FRET ratio was calculated by registering and dividing the FRET and donor images and calculating the ratio within the cell. Depletion was determined by a reduction in the normalized FRET ratio to below 0.8. (C) Untreated MLO-Y4 exhibited similar depletion characteristics as those treated with an L-Type inhibitor. Treatment with the T-Type inhibitor resulted in significantly faster depletion, quantified in the bar graph. (D) In MC3T3-E1, no differences were detected in the depletion times among all groups. Error bars are standard deviation. Significance was assessed by one-way ANOVA. *p<0.05 compared to control.

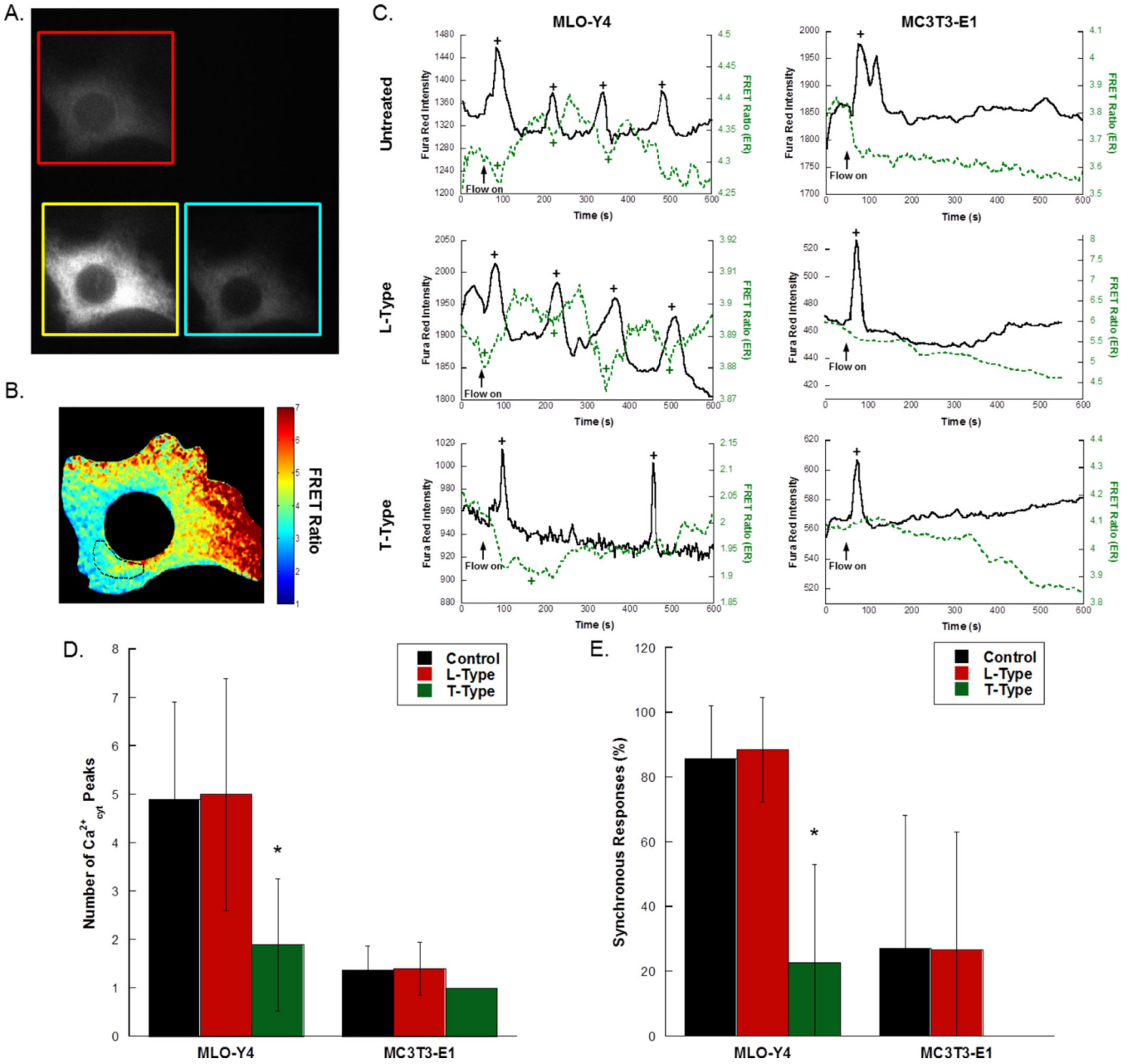

Figure 4. The effects of VSCC inhibitor treatment on Ca^{2+}_{cyt} responses and $Ca^{2+}_{cyt}/Ca^{2+}_{ER}$ synchrony in MLO-Y4 osteocytes and MC3T3-E1 osteoblasts

To simultaneously monitor Ca^{2+} in the cytosol and the ER, cells were transfected with D1ER and stained with the red-shifted fluorescent Ca^{2+}_{cyt} indicator Fura Red-AM. Single cells at 60× were imaged using a quadview beamsplitter with single excitation of both indicators to achieve simultaneous, real-time measurements of Ca^{2+}_{cyt} and Ca^{2+}_{ER}. A representative image is shown in (A). The FRET ratio was calculated from the FRET and donor images, and (B) shows the selection of a subregion to determine the changes in Ca^{2+}_{ER} microdomains corresponding to Ca^{2+}_{cyt} spike initiation. (C) Representative time courses from MLO-Y4 and MC3T3-E1 cells imaged at 60× magnification under fluid flow exposure in the presence or absence of L- and T-Type VSCC inhibitors. Flow was started

after the collection of 60s baseline. Detected peaks and valleys are indicated by "+". (D) The number of Ca^{2+}_{cyt} responses in untreated, L-Type inhibitor treated, and T-Type inhibitor treated bone cells. (E) The percentage of synchronous responses in MLO-Y4 and MC3T3-E1 treated with VSCC inhibitors. The percentage of synchronous responses was defined as the number of coincident Ca^{2+}_{cyt} and Ca^{2+}_{ER} transients divided by the total number of transients (peaks and inverse peaks). Error bars are standard deviation. Significance was assessed by multi-factorial ANOVA with Bonferroni's post hoc analysis. *$p<0.05$ compared to control.

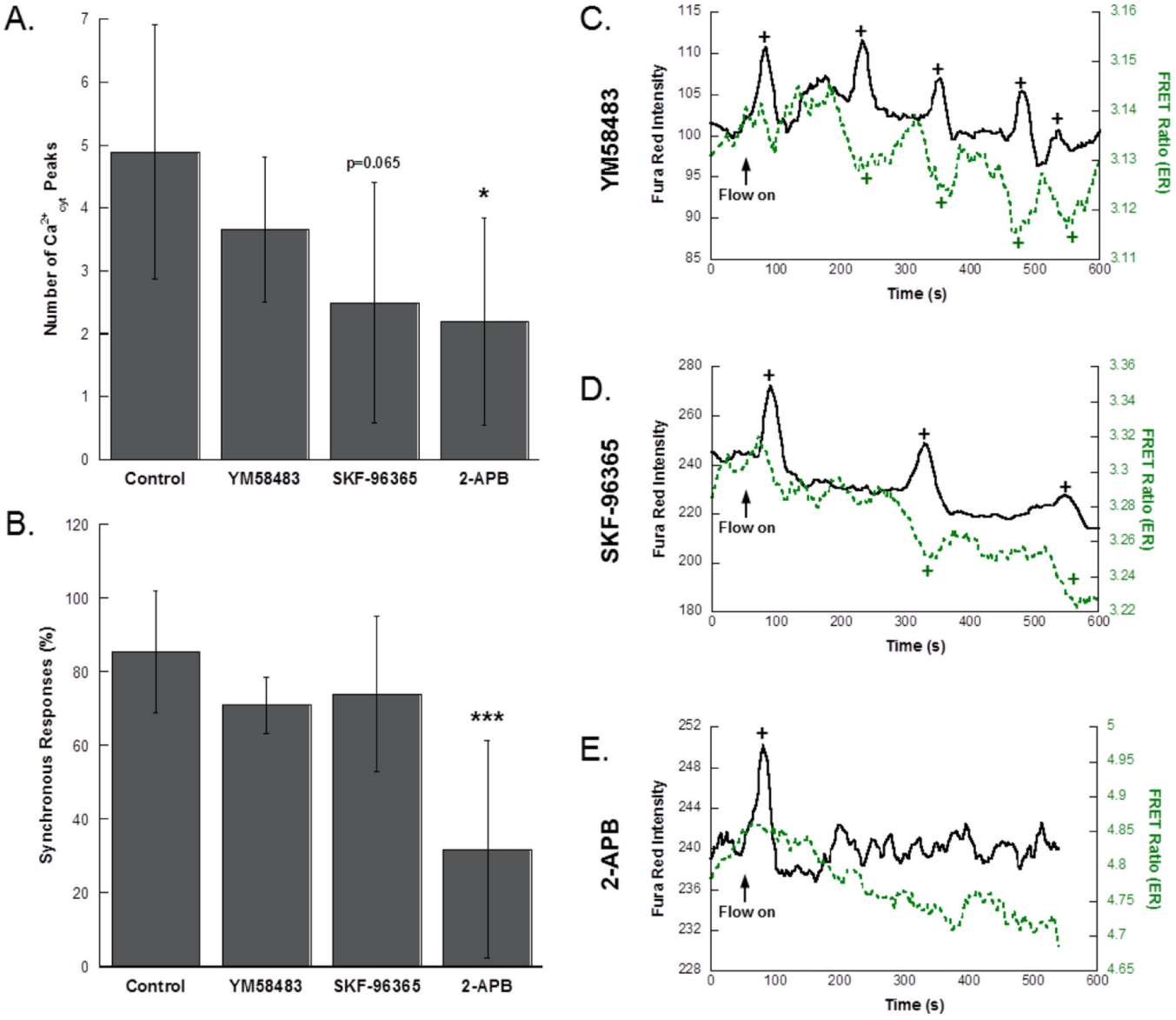

Figure 5. Pharmacologic inhibition of SOCE in MLO-Y4 osteocytes

(A) Number of Ca^{2+}_{cyt} peaks in control and inhibitor treated groups. (B) The percentage of synchronous responses in MLO-Y4 treated with SOCE inhibitors. Simultaneous measurement of Ca^{2+}_{cyt} and Ca^{2+}_{ER} in MLO-Y4 cells exposed to fluid shear pre-treated with (C) YM58483, (D) SKF-96365, and (E) 2-APB. Flow was started after the collection of 60s baseline. Detected peaks and valleys are indicated by "+". Significance was assessed by one-way ANOVA. Error bars are standard deviations. *p<0.05, ***p<0.001 compared to control.